Supporting Information

Geiger et al. 10.1073/pnas.0912021106

SI Text

Supplemental Text 1. To rule out that interactions arise from simple over-expression we performed control experiments with *G*uard cells *O*utward *R*ectifying K^+ channel (GORK). GORK is, like SLAC1, involved in stomatal closure. Channel function and expression of GORK is ABA sensitive (1, 2). In contrast to SLAC1 in coexpression experiments with oocytes, GORK together with OST1 did not show any fluorescence complementation in BIFC experiments (Fig. S5*b*).

Supplemental Text 2. Replacing aspartate at position 140 by alanine impairs the OST1 kinase activity. This position has been shown to play a crucial role in the active site as proton acceptor in protein kinases (consensus motif: HR***D***LKxxN; for review see ref. 3).

SI Methods

Real-Time PCR. Quantification of actin2/8 and SLAC1/OST1/ABI1-transcripts was performed by real-time PCR as described elsewhere (4). Transcripts were each normalized to 10,000 molecules of actin2/8. Primers used: AtACT2/8fwd 5′-GGT GAT GGT GTG TCT-3′, AtACT2/8rev 5′-ACT GAG CAC AAT GTT AC-3′, SLAC1fwd 5′-CCG GGC TCT AGC ACT CA-3′, SLAC1rev 5′-TCA GTG ATG CGA CTC TT-3′, ABI1fwd 5′-CTG CAA TAA CCA ATA CTC-3′, ABI1rev 5′-TCT TCT TCT CGC TAG TAA-3′, OST1fwd 5′-ACG ATA ACA CGA TGA C-3′, OST1rev 5′-TCC TGT GAG GTA ATG G-3′.

Cloning and cRNA Generation. The cDNA of SLAC1, OST1, SnRK2.2, 2.3, 2.8, ABI1, ABI2, HAB1 and HAB2 were cloned into oocyte (BIFC-) expression vectors (based on pGEM vectors) as well as in plant binary vectors (based on pCAMBIA vectors) by an advanced uracil-excision-based cloning technique described by Nour-Eldin et al. (5). Site-directed mutations were introduced with the quick-change site-directed mutagenesis kit according to the manufacturer's instructions (Stratagene/Agilent Technologies). For functional analysis cRNA was prepared using the mMessage mMachine T7 Transcription Kit (Ambion). Oocyte preparation and cRNA injection have been described elsewhere (6).

Oocyte Recordings. In TEVC experiments oocytes were perfused with Kulori-based solutions. The standard solution contained 10 mM Mes/Tris pH 5.6, 1 mM $CaCl_2$, 1 mM $MgCl_2$, 2 mM KCl, and 24 mM NaCl as well as 70 mM Na-gluconate. Solutions for selectivity measurements were composed of 50 mM Cl^-, HCO_3^-, SO_4^{2-}, NO_3^-, or malate$^-$ sodium salts, 85 mM Na-gluconate, 1 mM Ca-gluconate$_2$, 1 mM Mg-gluconate$_2$, 1 mM K-gluconate, as well as 10 mM Tris/Mes pH 5.6. Osmolality was adjusted to 220 mOsmol/kg using D-sorbitol. Steady state currents (I_{SS}) were extracted at the end of 15 s voltage pulses starting from a holding potential (V_H) of 0 mV and ranging from +60 to −180 mV in 10 mV decrements. The relative open probability P_o was determined from current responses to a constant voltage pulse to −120 mV subsequent to different test pulses. These currents were normalized to the saturation value of the calculated Boltzmann distribution. The half-maximal activation potential ($V_{1/2}$) and the apparent gating charge (z) were determined by fitting the experimental data points with a single Boltzmann equation. Instantaneous currents (I_t) were extracted right after the voltage jump from the holding potential to test pulses (500 ms) ranging from +60 to −180 mV in 10 mV decrements.

BIFC Experiments. Transient protoplast expression was performed using the polyethylene glycol transformation method modified after (7). Sixteen to 24 h after transformation protoplast images were taken. For documentation of the oocyte and protoplast BIFC (8) results, pictures were taken with a confocal laser scanning microscope (LSM 5 Pascal Carl Zeiss Jena GmbH.) equipped with a Zeiss Plan-Neofluar 20x/0.5 objective for oocyte images and a Zeiss Plan-Neofluar 63x/1.25 oil objective for protoplasts. Images were processed (low-pass filtered and sharpened) identically with the image acquisition software LSM 5 Pascal (Carl Zeiss).

Patch Clamp Experiments on Guard Cell Protoplasts. *Arabidopsis thaliana* ecotype Columbia (Col-0), *ost1–2 and slac1–3* mutants were grown on soil in a growth chamber at a 8/16 h day/night regime and 22/16 °C day/night temperature. Rosette leaves of 6–8 week-old plants were blended in ice-cold water 3 times for 20 s and washed with water through a 300-μm nylon mesh. The residual tissue was incubated for 18 h at 16–18 °C in enzyme solution composed of 0.65% (wt/vol) cellulase Onozuka-R10 (Serva), 0.35% (wt/vol) macerozyme Onozuka-R10 (Serva), 0.25% (wt/vol) bovine serum albumine (Serva), 0.05 mM KCl, 0.05 mM $CaCl_2$, 5 mM ascorbic acid, 0.05% (wt/vol) kanamycin sulfate (Fluka) and adjusted to pH 5.5/Tris and to an osmolality of 400 mosmol/kg with D-sorbitol. Afterward the enzyme treatment was continued at room temperature on a rotary shaker (75 rpm) for further 30 min. Then, the suspension was filtered through a 300-μm and 20-μm nylon mesh, washed with wash solution (400 mM sorbitol and 1 mM $CaCl_2$) and centrifuged at 100 × *g* and 4 °C for 12 min. The enriched protoplasts were stored on ice until aliquots were used for whole-cell patch clamp recordings of S-type anion currents which were performed essentially as described by (9, 10). The standard bath solution was composed of (in mM) 30 CsCl, 2 $MgCl_2$, 0.5 $LaCl_3$, and 10 Mes pH 5.6/Tris. For ABA activation of S-type currents the bath solution additionally contained 25 μM ABA, and protoplasts were preincubated in ABA (25 μM)-containing wash solution 20 to 30 min before patch clamping. The pipette solution consisted of (in mM) 150 TEA-Cl, 2 $MgCl_2$, 5 Mg-ATP, 5 Tris-GTP, 10 Hepes pH 7.1/Tris. To obtain a free Ca^{2+} concentration of 110 nM, the pipette solution additionally contained 10 mM EGTA plus 3 mM $CaCl_2$. The osmolality of the pipette and bath media was adjusted to 440 and 400 mosmol/kg, respectively, with D-sorbitol. Anion currents were measured 7 min after whole cell access and finally normalized off-line to the membrane capacitance (C_m) of the respective protoplast. For recording of ABA activated S-type anion currents, 7.5-s-lasting voltage pulses were applied from a holding voltage of +9 mV in the range from +44 to −136 mV in 30-mV decrements, followed by a 100-ms voltage pulse to -191 mV. The clamped voltages were corrected off-line for the liquid junction potential (11).

Protein Purification and in Vitro Kinase Assays. OST1, ABI1, and SLAC1 NT and CT were subcloned into the recombinant expression vector pGEX 6P1 (GE Healthcare) and transformed into *E. coli* (DE3) pLysS strain (Novagen). Bacteria were grown to OD 0.8 to 1.2 at 600 nm and production of GST-tagged proteins was induced by 0.4 mM isopropylthio-β-galatoside for 4 h at 25 °C. Cells were collected by centrifugation and then lysed

(in 50 ml PBS) by 3 20 s lasting sonication steps. To remove insoluble bacterial fractions the lysate was centrifuged for 20 min at 15,000 × *g*. Native purification using Glutathion-Sepharose 4 B beads (Amersham Biosciences) was performed in a batch procedure according to manufacturer's instructions; 50 mM Tris/HCl with 10 mM reduced glutathione was used for protein elution. Lysis and wash buffers were composed of 140 mM NaCl, 2.7 mM KCl, 10 mM Na_2HPO_4, and 1.8 mM KH_2PO_4 (pH 7.3). Proteins were dialyzed and stored in 50 mM Tris/HCl. In vitro kinase buffer was composed of 20 mM Hepes, pH 7.5, 0.5% (vol/vol) Triton X-100, 2 mM $MnCl_2$, 1 x protease inhibitor mixture (Roche), 10 mM NaF, 5 mM β-glycerophosphate and 5 mCi [Υ-^{32}P] ATP (3,000 Ci/mmol) (cf. ref. 9). Reactions were carried out for 15 min at room temperature and then stopped by adding 6 x SDS loading buffer and heating to 90 °C for 5 min. Proteins were separated by SDS-Gel electrophoresis using a 8 to 16% gradient acrylamide gel (Precise™ protein gel, Thermo Scientific) and detected by coomassie blue stain and autoradiography.

CelluSpots peptide arrays were ordered from Intavis Bioanalytical Instruments; 20 aa long peptides with 10 aa overlap at each end of SLAC1 N and C terminus were coupled to microscope slides by acetylation. To prevent nonspecific binding, the arrays were blocked by immersing the slides in 1 mg/ml BSA solution for 2 h at room temperature. The phosphorylation reaction was carried out for 2 h at room temperature by the use of 2 μg kinase, 5 mCi [Υ-^{32}P] ATP (3,000 Ci/mmol) and the in vitro kinase buffer described above. Subsequently slides were washed 3 to 4 times with PBS buffer containing 0.05% Tween-20. Phosphorylation was detected by autoradiography.

1. Becker D, et al. (2003) Regulation of the ABA-sensitive Arabidopsis potassium channel gene GORK in response to water stress. *FEBS Lett* 554:119–126.
2. Blatt MR, Gradmann D (1997) K(+)-sensitive gating of the K^+ outward rectifier in Vicia guard cells. *J Membr Biol* 158:241–256.
3. Hanks SK, Hunter T (1995) Protein kinases 6. The eukaryotic protein kinase superfamily: Kinase (catalytic) domain structure and classification. *FASEB J* 9:576–596.
4. Ivashikina N, et al. (2003) Isolation of AtSUC2 promoter-GFP-marked companion cells for patch-clamp studies and expression profiling. *Plant J* 36:931–945.
5. Nour-Eldin HH, Hansen BG, Norholm MH, Jensen JK, Halkier BA (2006) Advancing uracil-excision based cloning towards an ideal technique for cloning PCR fragments. *Nucleic Acids Res* 34:e122.
6. Becker D, et al. (1996) Changes in voltage activation, Cs^+ sensitivity, and ion permeability in H5 mutants of the plant K^+ channel KAT1. *Proc Natl Acad Sci USA* 93:8123–8128.
7. Abel S, Theologis A (1994) Transient transformation of Arabidopsis leaf protoplasts: A versatile experimental system to study gene expression. *Plant J* 5:421–427.
8. Walter M, et al. (2004) Visualization of protein interactions in living plant cells using bimolecular fluorescence complementation. *Plant J* 40:428–438.
9. Hamill OP, Marty A, Neher E, Sakmann B, Sigworth FJ (1981) Improved patch-clamp techniques for high-resolution current recording from cells and cell-free membrane patches. *Pflugers Arch* 391:85–100.
10. Ivashikina N, Deeken R, Fischer S, Ache P, Hedrich R (2005) AKT2/3 subunits render guard cell K^+ channels Ca^{2+} sensitive. *J Gen Physiol* 125:483–492.
11. Neher E (1992) Correction for liquid junction potentials in patch clamp experiments. *Methods Enzymol* 207:123–131.
12. Belin , et al. (2006) Identification of features regulating OST1 kinase activity and OST1 function in guard cells. *Plant Physiol* 141:1316–1327.

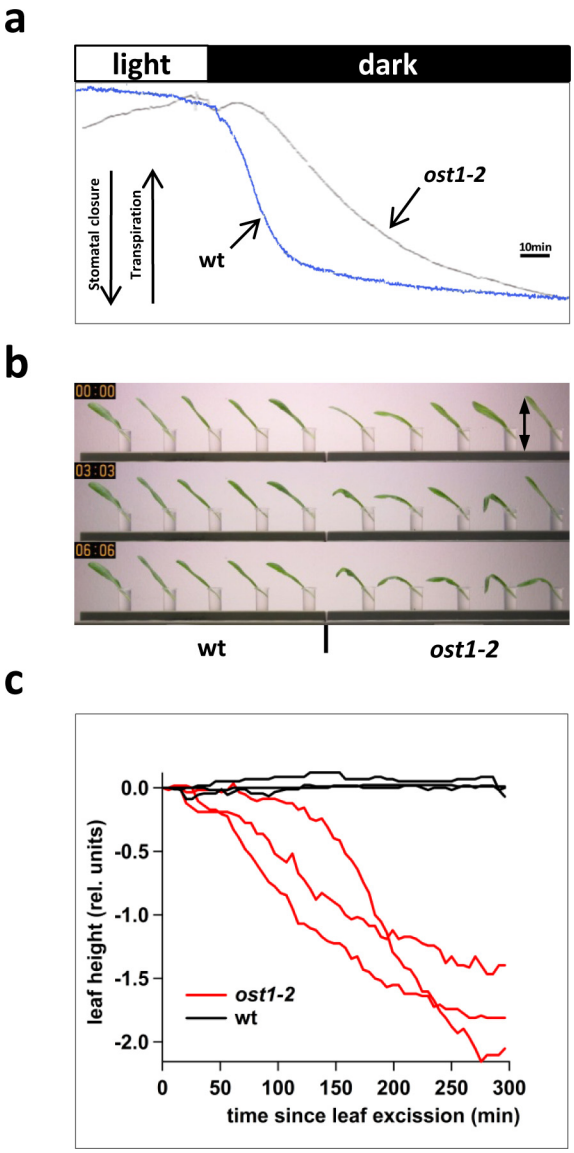

Fig. S1. *ost1–2* plants are unable to control stomatal closure. (*a*) Reduction in transpiration of *ost1–2* leaves upon light to dark transition is delayed. White and black bars indicate light and dark periods, respectively. Representative experiments are shown. (*b*) Wilting of *ost1–2* leaves in the light. Please note, that water feeding via the petiole does not prevent wilting of excised *ost1–2* leaves. The same leaves are shown at the indicated time points (See also Movie S1). (*c*) Time course of *ost1–2* leaves wilting compared to WT. The position of the leaf tip (see arrow in *b*) relative to the leaf base was plotted against time (after excision). Data from 3 individual *ost1–2* and 2 WT leaves each from different plants are shown.

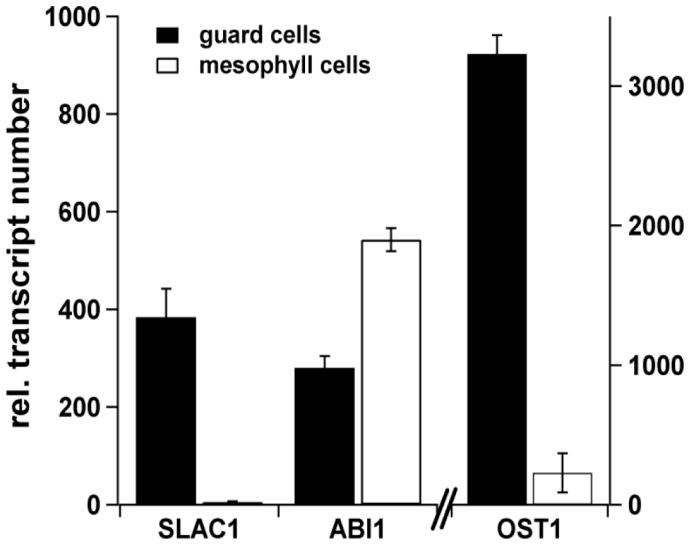

Fig. S2. Quantification of SLAC1, ABI1, and OST1 transcript levels in guard cells in comparison to mesophyll cells. Transcripts were normalized to 10,000 molecules of actin2/8 ($n = 4$, mean $\pm$ SD).

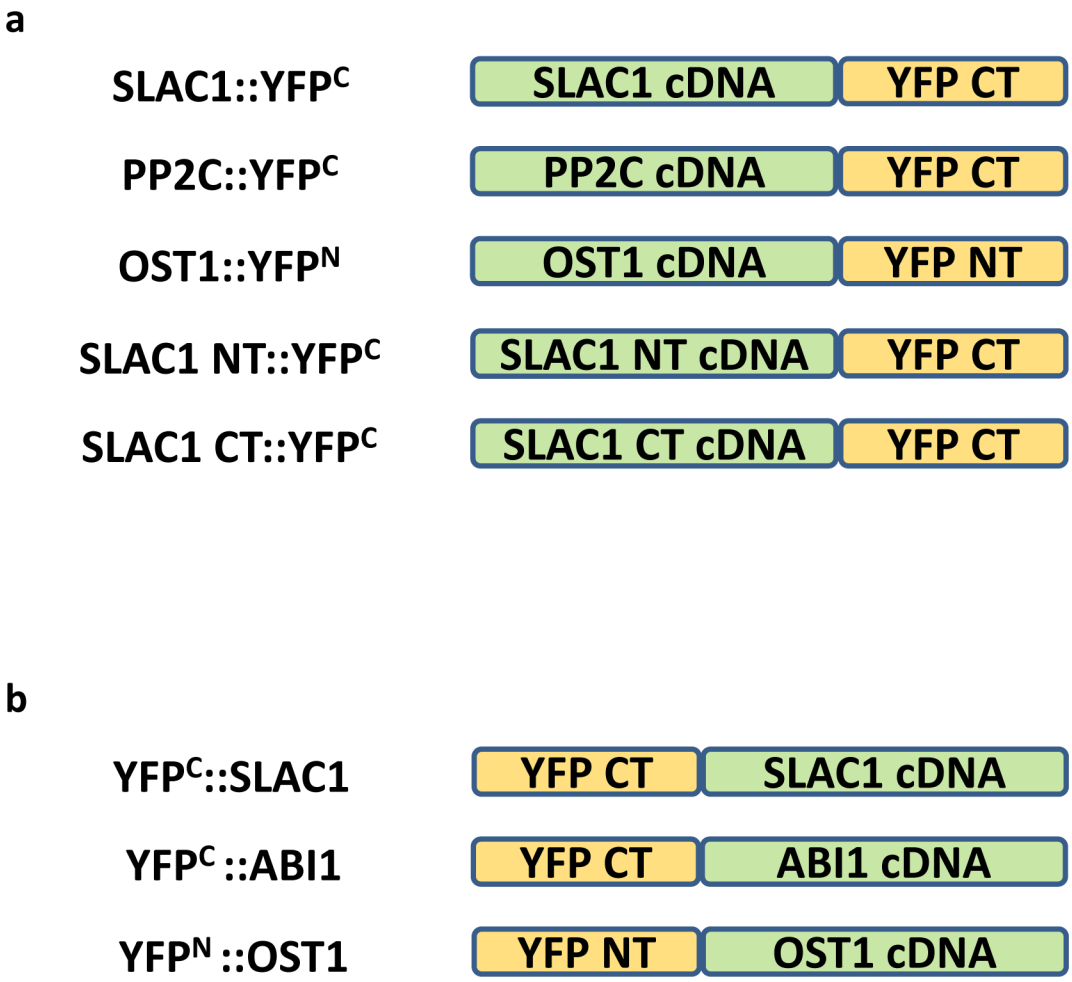

Fig. S3. Illustration of BiFC fusion constructs used in this study. (*a*) Fusion proteins used for oocytes BiFC recordings. (*b*) Fusion proteins used for interaction studies in *Arabidopsis* protoplasts by BiFC. (*a* and *b*) Abbreviations used in this study: YFP, yellow fluorescent protein; YFP^C, C-terminal half of YFP (amino acid 156 to 239); YFP^N, N-terminal half of YFP (amino acid 1 to 155); SLAC1 NT harbors amino acid 1 to 186; SLAC1 CT exhibits amino acid 496 to 556;

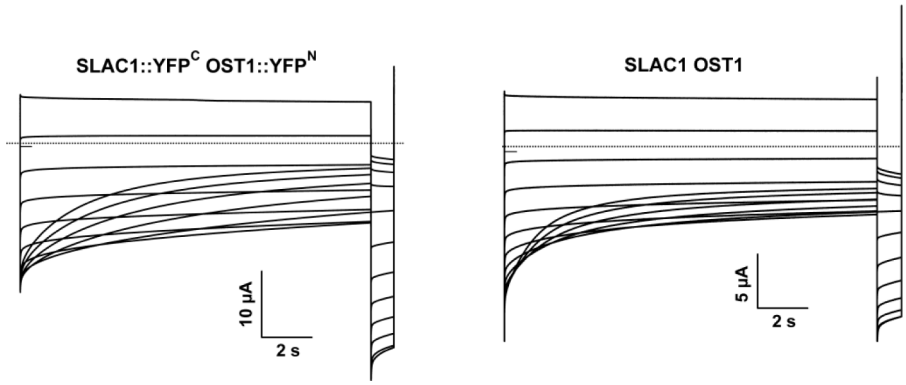

Fig. S4. Whole oocyte currents of a representative SLAC1::YFP^{C} OST1::YFP^{N} coexpressing oocyte (*Left*) compared to an oocyte expressing the native proteins (SLAC1 and OST1, *Right*) without split-YFP fusion. Note, electrical properties of the resulting currents were independent from the constructs (with or without split-YFP fusion) used for oocyte injection.

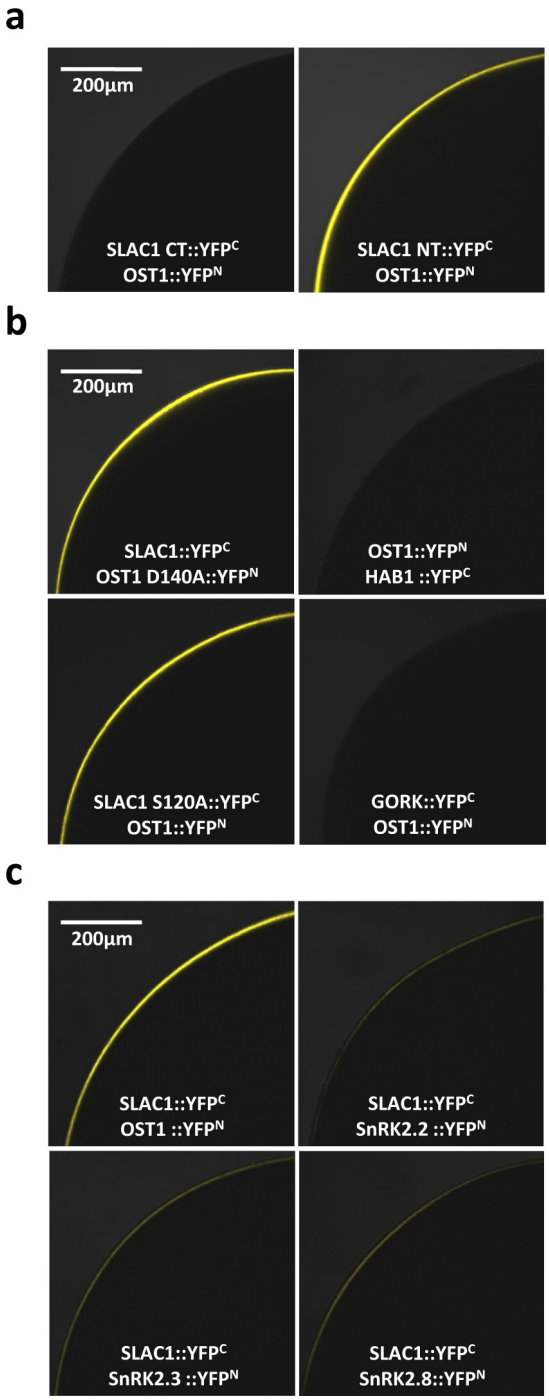

Fig. S5. A series of BiFC experiments in *Xenopus* oocytes identified interacting proteins. Pictures showing a quarter of an optical slice of an oocyte were taken with a confocal laser scanning microscope. The coinjected plasmids combinations are indicated in the figure. The C-terminal half of the YFP was fused to SLAC1 (termini of SLAC1 in *a*) whereas the N-terminal half of the YFP was fused to the kinases/phosphatases. Representative images are shown. (*a*) The N terminus of SLAC1 showed strong interaction with OST1, whereas SLAC1 CT OST1 coexpression lacked YFP fluorescence. OST1::YFP^N and HAB1::YFP^C did not result in YFP fluorescence. (*b*) Neither the disruption of the kinase activity of OST1 (D140A) nor the use of the SLAC1 mutant, S120A, prevented interaction with SLAC1 or OST1, respectively. BiFC control experiments with GORK coexpressed with OST1 did not result in YFP fluorescence. (*c*) Coexpression studies of SLAC1 with different members of the SnRK kinase family. Note that strongest BiFC signals were obtained with OST1.

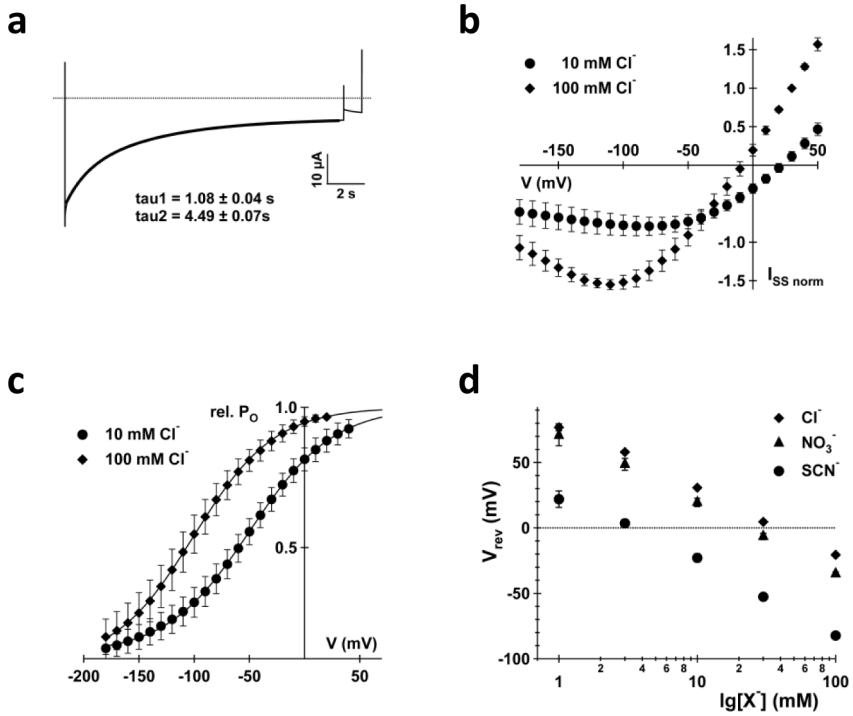

Fig. S6. Deactivation characteristics and anion dependency of SLAC1 currents. (*a*) A single 15 s voltage pulse to −180 mV starting from the holding potential of 0 mV in 30 mM external Cl^- was applied. The deactivation kinetics could be fitted with a double exponential equation, resulting in the indicated time constants. (*b*) SLAC1 steady-state currents (I_{SS}) normalized to the value at +30 mV in 100 Cl^- were plotted against the membrane voltage. Note the reduction of Cl^- efflux at negative membrane potentials ($n = 4$, mean ± SD). (*c*) The relative open probability (rel. P_O) of SLAC1 in 10 and 100 mM Cl^- was plotted against the membrane potential. The half-maximal activation potential ($V_{1/2}$) shifted to more negative potentials with increasing external Cl^- concentrations. Data points were fitted with a single Boltzmann equation (solid lines, $n = 4$, mean ± SD). (*d*) Reversal potentials for Cl^-, NO_3^- und SCN^- in the bath were shown as a function of the logarithmic external anion concentration. As expected for an anion-selective channel, the reversal potential shifted to more negative values with increasing anion concentrations ($n \geq 4$, mean ± SD). Experiments with SLAC1 activated by OST1 were performed with oocytes expressing SLAC1::YFP^C and OST1::YFP^N.

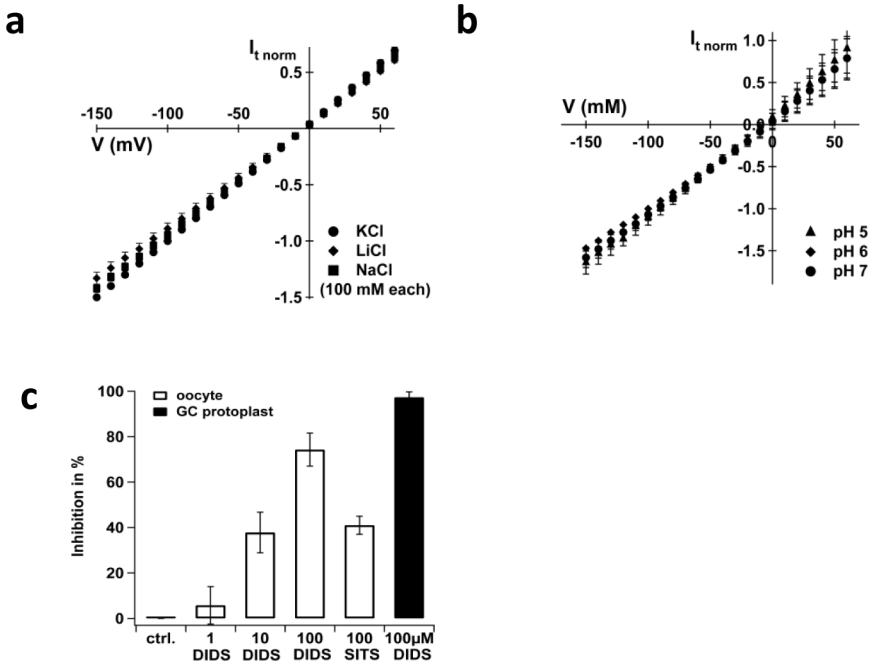

Fig. S7. (*a* and *b*) SLAC1 mediated instantaneous currents (I_t) were independent from the nature of external cations and the external proton concentration ($n \geq 3 \pm$ SD). I_t currents were normalized to currents at −100 mV at pH 5 and 100 mM KCl (in a) or 100 mM KCl, pH 5.5 (in *b*). (*c*) Percentage of SLAC1 current inhibition in oocytes by the anion channel inhibitors DIDS and SITS at the indicated inhibitor concentrations (open bars, $n = 4$). The black bar shows the inhibition of SLAC1-like currents in *Arabidopsis* guard cell protoplasts (WT) by 100 μM DIDS ($n = 3$). Current inhibition was determined in oocytes at −100 mV and in protoplasts at −96 mV. Experiments with SLAC1 activated by OST1 were performed with oocytes expressing SLAC1::YFP^C and OST1::YFP^N.

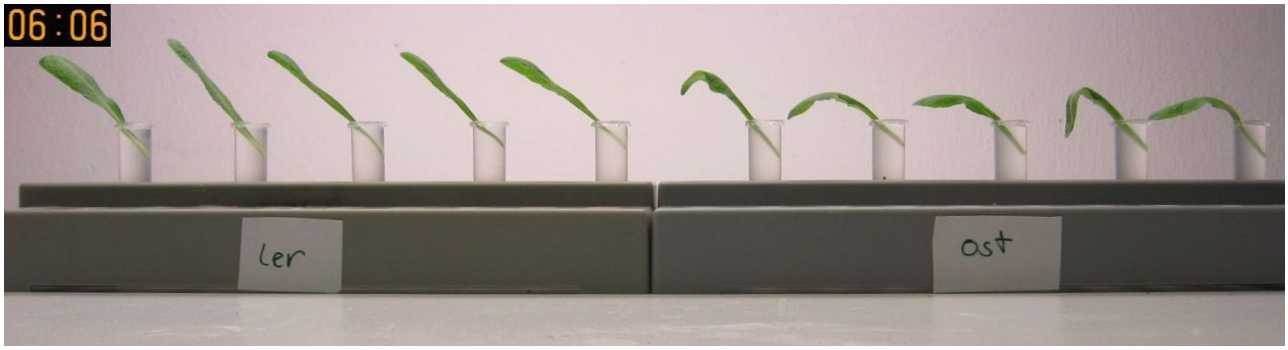

Movie S1. Excised leaves from 6 to 8 week old WT (Ler) and *ost1–2* plants were put into a 1.5 ml reaction cup filled with water. The movie spanned 6 h in the light. In contrast to WT leaves, *ost1–2* leaves could not properly adjust their stomatal aperture in response to ongoing water- and turgor loss. This resulted in premature wilting of *ost1–2* leaves relative to WT leaves.

Movie S1 (AVI)

Table S1. CelluSpots peptide arrays were used to identify putative phosphorylation sites within the N- and C-terminal part of SLAC1. Thereby phosphorylation by OST1 was detected by the use radio-labeled [γ^{32}] ATP and subsequent autoradiography. + indicates peptides which were (weakly) phosphorylated. ++ indicates peptides which showed high phosphorylation signals

SLAC1 NT	aa position	aa sequence	Phosphorylation
	1to 20	MERKQSNAHSTFADINEVED	−
	11to 30	TFADINEVEDEAEQELQQQE	−
	21to 40	EAEQELQQQENNNNKRFSGN	−
	31to 50	NNNNKRFSGNRGPNRGKQRP	−
	41to 60	RGPNRGKQRPFRGFSRQVSL	+
	51to 70	FRGFSRQVSLETGFSVLNRE	−
	61to 80	ETGFSVLNRESRERDDKKSL	−
	71to 90	SRERDDKKSLPRSGRSFGGF	+
	81to100	PRSGRSFGGFESGGIINGGD	−
	91to110	ESGGIINGGDGRKTDFSMFR	−
	101to120	GRKTDFSMFRTKSTLSKQKS	++
	111to130	TKSTLSKQKSLLPSIIRERD	++
	121to140	LLPSIIRERDIENSLRTEDG	−
	131to150	IENSLRTEDGETKDDSINEN	−
	141to160	ETKDDSINENVSAGRYFAAL	−
	151to170	VSAGRYFAALRGPELDEVKD	−
	161to180	RGPELDEVKDNEDILLPKEE	−
	171to186	NEDILLPKEEQWPFLL	−
SLAC1 CT			
	496to515	HAFVWQTLFPNDLAIAITKR	−
	506to525	NDLAIAITKRKLTREKKPFK	+
	516to535	KLTREKKPFKRAYDLKRWTK	−
	526to545	RAYDLKRWTKQALAKKISAE	−
	536to555	QALAKKISAEKDFEAEEESH	−
	546to556	KDFEAEEESHH	−